Fabrication of $CoFe_2O_4$ ferrite nanowire arrays in porous silicon template and their local magnetic properties*

Hui Zheng(郑辉), Man-Gui Han(韩满贵)†, and Long-Jiang Deng(邓龙江)

State Key Laboratory of Electronic Thin Films and Integrated Devices, University of Electronic Science and Technology of China, Chengdu 610054, *China*

(Received 27 June 2015; revised manuscript received 1 November 2015; published online 10 January 2016)

$CoFe_2O_4$ ferrite nanowire arrays are fabricated in porous silicon templates. The porous silicon templates are prepared via metal-assisted chemical etching with gold (Au) nanoparticles as the catalyst. Subsequently, $CoFe_2O_4$ ferrite nanowires are successfully synthesized into porous silicon templates by the sol–gel method. The magnetic hysteresis loop of nanowire array shows an isotropic feature of magnetic properties. The coercivity and squareness ratio (M_r/M_s) of ensemble nanowires are found to be 630 Oe (1 Oe = 79.5775 A·m^{-1} and 0.4 respectively. However, the first-order reversal curve (FORC) is adopted to reveal the probability density function of local magnetostatic properties (i.e., interwire interaction field and coercivity). The FORC diagram shows an obvious distribution feature for interaction field and coercivity. The local coercivity with a value of about 1000 Oe is found to have the highest probability.

Keywords: ferrite nanowires, porous silicon, metal-assisted chemical etching, first order reversal curves

PACS: 62.23.Hj, 68.65.–k, 75.30.Gw **DOI:** 10.1088/1674-1056/25/2/026201

1. Introduction

Recently, one-dimensional (1D) magnetic structures, especially magnetic nanowire arrays, have attracted much attention due to their unique potential applications in magnetic integrated nanosystems, perpendicular magnetic records, microwave absorbing and spintronic nanodevices.[1–4] Cobalt spinel ferrite $CoFe_2O_4$ (CFO) is well known for its high coercivity, giant magnetostriction, unique light-induced coercivity change, and remarkable chemical stability. CFO has various applications, such as humidity sensors, photodetectors, biomedical, magnetoelectric devices.[5–7] Lately, it was reported that magnetic nanowires can be fabricated by many approaches such as electrospinning, sol–gel, hydrothermal and electrodeposition methods.[8–10] Pirouzfar *et al.* have synthesized CFO nanowires with high coercivity values via the sol–gel route by using anodized aluminum oxide (AAO) as template.[9] Besides, Xu *et al.* have fabricated CFO nanowires with the preferred crystalline orientation along the length direction of nanowires by electrodeposition in AAO templates.[10] As shown in these studies, most CFO nanowire arrays or other ferrite nanowire arrays were fabricated in AAO templates.[11,12] However, the AAO templates are very fragile and easy to break into pieces, which are required to be handled with special caution. Therefore, it makes them extreme difficult to be assembled into sturdy devices. Currently, there is a trend towards incorporating many functions into silicon substrates, such as systems on chips.[4,13] Therefore, it is very important to be capable of fabricating CFO nanowire array in silicon, which will be compatible with semiconductor industry in future for the integrated nanosystems. In this paper, we report the fabrication of CFO nanowire array on silicon substrate and its magnetic properties. To the best of our knowledge, no one else has done this before. Since porous silicon was discovered,[14] it has attracted lots of attention due to its potential applications in optoelectronics, chemical and biochemical sensing devices.[15,16] Usually, porous Si is prepared by electrochemical etching under anodic bias in fluoride-containing solutions.[17] Recently, a new method based on metal-assisted chemical etching has attracted increasing attention for its simplified and low-cost fabricating process.[18,19] In this paper, we first prepare the porous silicon templates by a technique named metal-assisted chemical etching through using Au nanoparticles as the catalysts. Then the CFO nanowire arrays are fabricated into the channel of porous silicon by the sol–gel method. The local magnetic properties of CFO nanowire arrays have been investigated by taking the first order reversal curve (FORC). The conventional magnetic hysteresis loop taken by a conventional magnetometry, such as vibrating sample magnetometry (VSM), usually shows the ensemble average properties over a whole sample. Especially there are more than millions of nanoscale elements in a nanodot (or nanowire) array, and the variations of magnetic properties of individual elements (such as coercivity, switching fields) are essentially important. Using the FORC method, much meaningful information about these variations can be obtained such as the distribution of magnetic properties, the quantitative phase analysis of mixed magnetic phases materials and distinguishing the reversible and irreversible magnetization switching

*Project supported by the National Natural Science Foundation of China (Grant No. 61271039), the Scientific Projects of Sichuan Province, China (Grant No. 2015HH0016), and the Natural Science Foundations of Zhejiang Province, China (Grant Nos. LQ12E02001 and Y107255).

†Corresponding author. E-mail: magnet@uestc.edu.cn

© 2016 Chinese Physical Society and IOP Publishing Ltd

processes.[20–23]

2. Experimental details

2.1. Preparation of porous silicon template

Single crystalline p-type silicon (200 Ω·cm) wafers were successively washed by immersing into acetone for 10 min, ethyl alcohol for 10 min and 5% HF for 5 min, which can remove the organic contaminants and a thin silicon dioxide layer. Polystyrene-block-poly(2-vinylpyridine) (PS-b-P2VP) diblock copolymer ($M_{n,NMR} = 1.2 \times 10^4$ g/mol, PS_{20}-b-$P2VP_{190}$) was synthesized in our laboratory, and it was dissolved in toluene to form a 5-mg/ml solution. Subsequently, the experiments were carried out in three steps, which were schematically shown in Fig. 1. Firstly, PS-b-P2VP thin films were formed on the silicon substrates by spin coating at room temperature, typically at 5000 rpm and 30 s. The coated silicon substrate was then immersed in the $HAuCl_4$ solution (5 mg/mL) with methanol for 2 min to load $HAuCl_4$ solution into the P2VP cores. Then the $HAuCl_4$-loaded film was immersed into the sodium citrate solution (0.03 M) at 60 °C for 15 min to reduce $HAuCl_4$ precursors into Au nanoparticles in the P2VP cores. Secondly, the thin film containing Au nanoparticles was heated with an alcohol lamp for 25 min to remove the organic copolymers. Thirdly, after obtaining the ordered Au nanoparticle on the silicon surface, the silicon wafer was etched in an aqueous solution containing HF, H_2O_2 and H_2O (HF/H_2O_2/H_2O = 1/5/10, volume ratio) at 60 °C for 1 h.

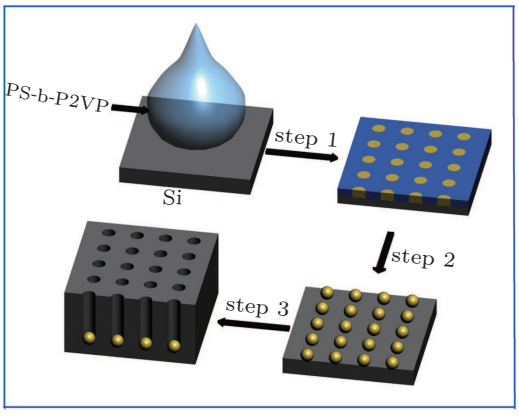


Fig. 1. (color online) Schematic procedures of preparation of porous silicon template.

2.2. Preparation of $CoFe_2O_4$ nanowires

Metal nitrates were used as the cationic sources, and citric acid and polyethylene glycol (PEG 20000) as the monomers for forming the polymeric matrix. Citric acid and PEG were dissolved in deionized water by stirring at 80 °C to make the first solution. $Co(NO_3)_2{\cdot}6H_2O$ and $Fe(NO_3)_3{\cdot}9H_2O$ were dissolved in deionized water with a molar ratio of 1:2, and then mixed with the first solution. The molar ratio of total nitrates to citric acid was 1:1. The weight ratio of $CoFe_2O_4$ to PEG was 1:2. The final solution was stirred at 80 °C for 3 h to induce esterification and form a sol. The porous Si template was immersed in this sol with the aid of ultra sound. The sol in the porous Si template was dried in air at 80 °C for 1 h. Excess sol on the template surface was carefully wiped off and then was sintered in a furnace at 800 °C for 1 h.

2.3. Characterizations of porous Si and $CoFe_2O_4$ nanowire

The morphologies of Au nanoparticles, $CoFe_2O_4$ nanowire, surface, and cross section of porous Si template were investigated by a scanning electron microscope (SEM). The composition of CFO nanowires was checked by an energy dispersive spectrometer (EDS). The phase of nanowires was examined by x-ray diffraction (Cu K_α radiation). The static magnetic properties were investigated by a vibrating sample magnetometer (VSM). Using the conventional VSM, the FORC method requires to take a series of partial hysteresis curves (FORC curves), which fill the interior of a major hysteresis loop of sample. For each FORC curve, the sample was firstly saturated at a large positive field (H_s). Subsequently, the applied field was reduced to a reversal field (H_a), the sample was saturated again starting from H_a. The magnetization of each applied field (H_b) on the FORC curve is denoted as $M(H_a, H_b)$. For a set of FORC measurements, it must be noted that the field spacing should be equal (i.e., $\Delta H_b = \Delta H_a$). According to the statistical model (called "Preisach model") which describes a set of hysterons that constitute a major hysteresis loop, the probability density function $\rho(H_a, H_b)$ (also called FORC distribution) of the hysterons ensemble can be calculated by the following mixed second derivative:

$$\rho(H_a, H_b) = -\frac{1}{2}\frac{\partial^2 M}{\partial H_a \partial H_b}. \quad (1)$$

To study the local static magnetic properties, the FORC distribution is often plotted in the coordinate system (H_u, H_c), where H_u is the local interaction field and H_c is the local coercivity. The relationships between two coordinate systems (H_a, H_b) and (H_u, H_c) are given as $H_c \equiv (H_b - H_a)/2$ and $H_u \equiv (H_a + H_b)/2$.

3. Results and discussion

PS-b-P2VP consists of a nonpolar PS block covalently linked to a polar P2VP domain. It spontaneously forms a monodisperse PS corona and P2VP core micelles in toluene which is a selective solvent for the PS block and nonselective solvent for P2VP. When it is coated by spin coating onto the clean silicon wafer with a rotation speed of 5000 rpm, the polymer molecules are self-assembled into a thin film with P2VP nano domains surrounded by PS corona.[24] Once the

PS-b-P2VP thin film is immersed into $HAuCl_4$ solution with methanol (a selective solvent for the P2VP core), core-corona inversion is induced in-situ without ruining the film.[25] The $HAuCl_4$ is then loaded into the P2VP due to the pyridine complexing reaction.[26] Subsequently, the Au nanoparticles can be obtained by reducing the $HAuCl_4$ solution in the sodium citrate solution. Finally, the polymer layer is removed with an alcohol lamp without disturbing the nanoparticle pattern.[27,28] In our experiments, the arrangement of Au nanoparticles on the silicon surface is shown in Fig. 2(a). As shown in the figure, the mean diameter of Au nanoparticles is 50±10 nm, which determines the minimum pore size of porous silicon template.

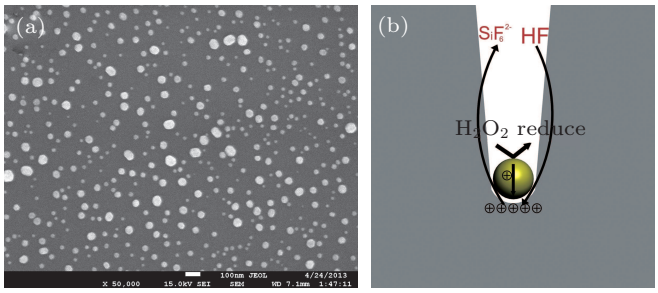


Fig. 2. (color online) (a) Arrangement of Au nanoparticles on the surface of silicon template, and (b) mechanism of porous silicon preparation by metal assisted chemical etching.

After the array of Au nanoparticles is obtained, the silicon template with the surface modified by Au is immersed into an aqueous solution containing HF and H_2O_2. The mechanism of the Au-assisted chemical etching is illustrated in Fig. 2(b). It is well accepted that the chemical or electrochemical reactions occur preferentially near an Au nanoparticle. At a cathode site, H_2O_2 is reduced at the metal surface through the following reaction:

$$\text{Cathode reaction:} \quad H_2O_2 + 2H^+ \rightarrow 2H_2O + 2h^+. \qquad (2)$$

Simultaneously, the injection of holes into silicon through the metal takes place. At an anode site, silicon is oxidized and dissolved. The anodic reaction can be indicated by the following equation:

$$\text{Anode reaction:}$$
$$Si + 6HF + nh^+ \rightarrow nH_2O + H_2SiF_6 + \frac{4-n}{2}H_2\uparrow, \qquad (3)$$

where n is the number of holes per dissolved silicon atom. Taking into account the cathodic reduction of H_2O_2, the overall chemical reaction can be expressed as[29–31]

$$\text{Overall reaction:}$$
$$Si + 6HF + \frac{n}{2}H_2O_2 \rightarrow H_2SiF_6 + nH_2O + \left[\frac{4-n}{2}\right]H_2\uparrow. \qquad (4)$$

The size of the pores of a porous silicon template can be controlled by the concentration ratio between HF and H_2O_2 in the etching solution, etching temperature and etching time. Under our optimized etching condition, the Au-modified silicon is treated at 60 °C for 1 h in the etching solution containing HF, H_2O_2, and H_2O (HF: H_2O_2: H_2O = 1:5:10, volume ratio). The obtained porous silicon template is shown in Fig. 3. Figure 3(a) shows the top view of template. It can be seen that many nanoscale pores have been obtained by the etching procedures. The sizes and spacings of pores are found not uniform. The size of the pore is found to be larger than that of Au nanoparticle, which indicates that the etching process takes place not only in the longitudinal direction, but also in the transverse direction. The cross section of a porous silicon template is shown in Fig. 3(b). Clearly, the channel of pore is straight. The length of pore channel is about 400 μm.

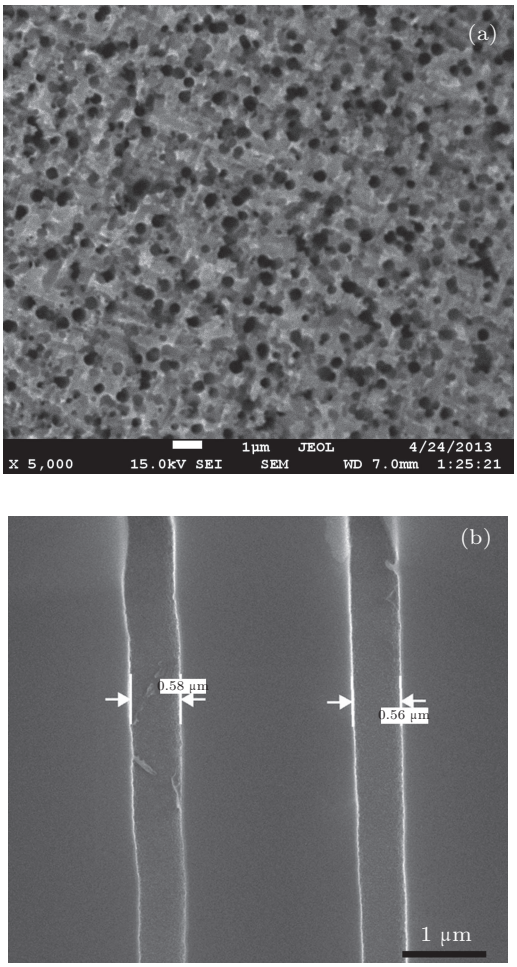


Fig. 3. SEM images of (a) top view and (b) cross section view of porous silicon template.

The CFO nanowires are shown in Figs. 4(a)–4(d). Single nanowires are shown in Figs. 4(a) and 4(c). The nanowire arrays are shown in Figs. 4(b) and 4(d) after the porous silicon template has been dissolved away. It is seen that the CFO nanowires fabricated by the sol–gel approach are straight, well crystallized and smooth in the pores of porous silicon. The diameter of the nanowire is measured to be about 200 nm, which

is smaller than the diameter of pore (see Fig. 4(a)). It is believed that the volume reduction of CFO nanowire is due to the evaporation of water and citric acid during calcination at 800 °C. From the perspective of CFO sensors, the interspace between the CFO nanowire and template is helpful to increase the sensing surface. It can also be seen in Fig. 4(d) that the diameters of nanowires are nearly homogeneous. The composition of the nanowire has been examined by the EDS measurements as shown in Fig. 5. Clearly, Fe, Co, and O elements are identified. The detected silicon element is from the silicon template. The XRD pattern of porous silicon template embedded with CFO nanowires is shown in Fig. 6. It can be learned that CFO nanowires are well crystallized, and single spinel phase is found for the obtained CFO nanowire array. No other phases are detected.

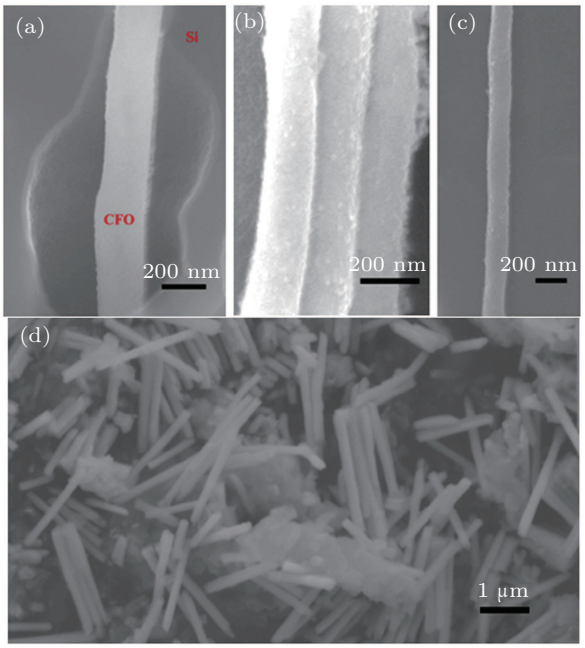


Fig. 4. (color online) (a)–(d) SEM images of $CoFe_2O_4$ nanowires.

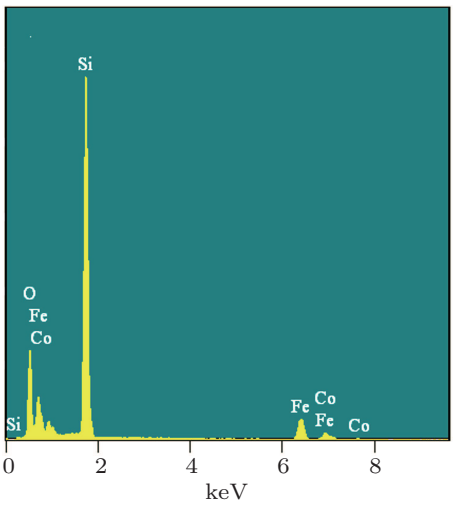


Fig. 5. (color online) Composition analysis of $CoFe_2O_4$ nanowire array.

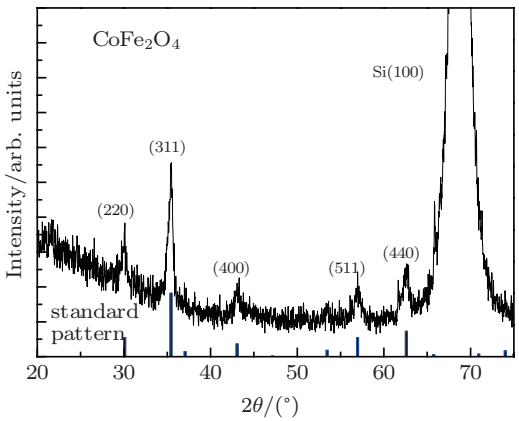


Fig. 6. XRD pattern of $CoFe_2O_4$ nanowires array.

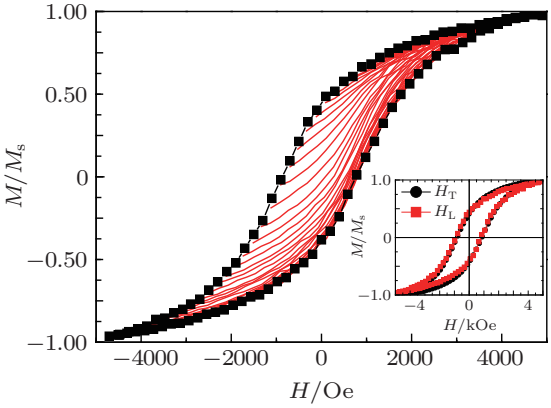


Fig. 7. (color online) First order reversal curves of $CoFe_2O_4$ nanowire arrays. Hysteresis loops in the inset are measurements in two different directions of applied field.

The static magnetic properties of CFO nanowires in porous templates are studied by using the hysteresis loops as shown in Fig. 7. The hysteresis loops are obtained with the applied magnetic fields along the longitudinal (H_L) and the transverse (H_T) direction of nanowires. It is shown that their hysteresis loops are almost identical, which means that the CFO nanowires fabricated each show an isotropic behavior see the inset in Fig. 7. The coercivity (H_c) of CFO nanowire array is found to be 630 Oe. The squareness ratio (M_r/M_s) is about 0.4. As mentioned before, the FORC method can be used to study the local magnetic properties for nanostructured materials. For our studies of $CoFe_2O_4$ nanowire array, the FORC diagram is shown in Fig. 8(a). Obviously, the distributions of coercivity values and inter-wire interactions are wide. Among some nanowires, there are no magnetic interactions. For some nanowire elements, the interaction is positive. For other nanowire elements, the interaction is negative. To show the distribution of coercivity values, the profile of coercivity with zero magnetic interaction (i.e. $H_u = 0$) is shown in Fig. 8(b). It is interesting to show that the coercivity value varies from 200 Oe to 3000 Oe. The coercivity with a value about 1000 Oe has a highest probability as depicted in Fig. 8(b). The observed distributions of H_u and H_c are due

to the inhomogeneous responses of nano elements to the applied magnetic field. Besides, the dimensional differences, i.e., differences in the diameter and spacing of nanowires) among nanowires are the other cause. As shown in Fig. 3, the nanopore sizes and spacings are not identical, which will also result in the observed distributions of H_u and H_c values.

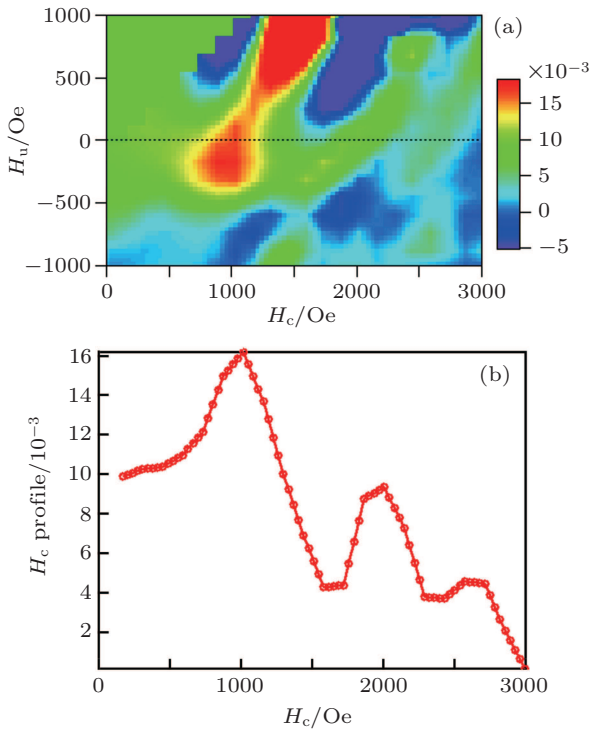


Fig. 8. (color online) (a) FORC diagrams of $CoFe_2O_4$ array, and (b) coercivity profile.

4. Conclusions

In this study, cobalt spinel ferrite nanowires are synthesized by a sol–gel method into the porous silicon template which is fabricated by the Au-assisted chemical etching procedure. It is found that the pore size is dependent on the size of Au nanoparticle. The spacing between nanopores is dependent on the spacing between Au nanoparticles on silicon substrate. For the ensemble CFO nanowires, conventional hysteresis loops show that the magnetic properties of CFO nanowire array in porous silicon template are isotropic. However, the FORC diagram derived from a series of first order reversal curves shows the wide distributions of local magnetic properties (H_u and H_c). For instance, the local coercivity with a value of about 1000 Oe is found to have the highest probability. The inhomogeneity of pore sizes and pore spacings is one of the causes responsible for the distribution of local magnetic properties.

References

[1] Gudiksen M S, Lauhon L J, Wang J, Smith D C and Lieber C M 2002 *Nature* **415** 617
[2] Zhang S Y, Xiu X Q, Hua X M, Xie Z L, Liu B, Chen P, Han P, Lu H, Zhang R and Zheng Y D 2014 *Chin. Phys. Lett.* **31** 056802
[3] Lu H P, Han M G, Cai L and Deng L J 2011 *Chin. Phys. B* **20** 060701
[4] Wang Z W, Cai J Q, Wu Y Z, Wang H J and Xu X L 2015 *Chin. Phys. B* **24** 017802
[5] Jia Z G, Yang L L, Wang Q Z, Liu J H, Ye M F and Zhu R S 2014 *Mater. Chem. Phys.* **145** 116
[6] Li X H, Xu C L, Han X H, Qiao L, Wang T and Li F S 2010 *Nanoscale Res. Lett.* **5** 1039
[7] Petrov V M, Bichurin M I and Srinivasan G 2010 *J. Appl. Phys.* **107** 073908
[8] Ramulu T S, Venu R, Anandakumar S, Sudha Rani V, Yoon S S and Kim C G 2012 *Thin Solid Films* **520** 5508
[9] Pirouzfar A and Seyyed Ebrahimi S A 2014 *J. Magn. Magn. Mater.* **370** 1
[10] Xu Y, Xue D S, Gao D Q, Fu J L, Fan X L, Guo D W, Gao B and Sui W B 2009 *Electrochim. Acta* **54** 5684
[11] Hua Z H, Chen R S, Li C L, Yang S G, Lu M, Gu B X and Du Y W 2007 *J. Alloys Compnd.* **427** 199
[12] Gu J J, Han J R, Cheng F W, Zhao G L, Liu L H and Sun H Y 2012 *Acta Phys. Sin* **61** 097502 (in Chinese)
[13] Adeyeye A O and Singh N 2008 *J. Phys. D: Appl. Phys.* **41** 153001
[14] Uhlir A 1956 *Bell Syst. Tech. J.* **35** 333
[15] Nicewarner-Pena S R, Freeman R G, Reiss B D, He L, Pena D J, Walton I D, Cromer R, Keating C D and Natan M J 2001 *Science* **294** 137
[16] Zheng H, Han M G, Deng J X, Zheng L, Wu J, Deng L J and Qin H B 2014 *Appl. Surf. Sci.* **311** 672
[17] Huang Z P, Zhang X X, Reiche M, Liu L F, Lee W, Shimizu T, Senz S and Gösele U 2008 *Nano Lett.* **8** 3046
[18] Kim J K, Han H, Kim Y H, Choi S H, Kim J C and Lee W 2011 *ACS Nano* **5** 3222
[19] Zheng H, Zhou J J, Deng J X, Zheng P, Zheng L, Han M G, Yang Y Q, Deng L J and Qin H B 2014 *Mater. Lett.* **123** 181
[20] Pike C R, Roberts A P and Verosub K L 1999 *J. Appl. Phys.* **85** 6660
[21] Davies J E, Wu J, Leighton C and Liu K 2005 *Phys. Rev. B* **72** 134419
[22] Béron F, Pirota K R, Vega V, Prida V M, Fernández A, Hernando B and Knobel M 2011 *New J. Phys.* **13** 013035
[23] Pike C R, Ross C A, Scalettar R T and Zimanyi G 2005 *Phys. Rev. B* **71** 134407
[24] Zu X H, Tu W P and DengY L 2011 *J. Nanopart. Res.* **13** 1
[25] Jennifer Q Lu and Yi S S 2006 *Langmuir* **22** 3951
[26] Polleux J, Rasp M, Louban I, Plath N, Feldhoff A and Spatz J P 2011 *ACS Nano* **5** 6355
[27] Glass R, Moller M and Spatz J P 2003 *Nanotechnology* **14** 1153
[28] Huang Z P, Geyer N, Liu L F and Zhong P 2010 *Nanotechnology* **21** 465301
[29] Yae S J, Morii Y, Fukumuro N and Matsuda H 2012 *Nanoscale Res. Lett.* **7** 352
[30] Chartier C, Bastide S and Levy-Clement C 2008 *Electrochimica Acta* **53** 5509
[31] Huang Z P, Shimizu T, Senz S, Zhang Z, Zhang X X, Lee W, Geyer N and Gosele U 2009 *Nano Lett.* **9** 2519